Journal of Biomedical Optics

BiomedicalOptics.SPIEDigitalLibrary.org

Ultrasensitive, real-time analysis of biomarkers in breath using tunable external cavity laser and off-axis cavity-enhanced absorption spectroscopy

Ismail Bayrakli
Hatice Akman

SPIE.

Ultrasensitive, real-time analysis of biomarkers in breath using tunable external cavity laser and off-axis cavity-enhanced absorption spectroscopy

Ismail Bayrakli* **and Hatice Akman**
Suleyman Demirel University, Biomedical Engineering, Batı Yerleşkesi E14 Blok, Isparta, Turkey

Abstract. A robust biomedical sensor for ultrasensitive detection of biomarkers in breath based on a tunable external cavity laser (ECL) and an off-axis cavity-enhanced absorption spectroscopy (OA-CEAS) using an amplitude stabilizer is developed. A single-mode, narrow-linewidth, tunable ECL is demonstrated. A broadly coarse wavelength tuning range of 720 cm^{-1} for the spectral range between 6890 and 6170 cm^{-1} is achieved by rotating the diffraction grating forming a Littrow-type external-cavity configuration. A mode-hop-free tuning range of 1.85 cm^{-1} is obtained. The linewidths below 140 kHz are recorded. The ECL is combined with an OA-CEAS to perform laser chemical sensing. Our system is able to detect any molecule in breath at concentrations to the ppbv range that have absorption lines in the spectral range between 1450 and 1620 nm. Ammonia is selected as target molecule to evaluate the performance of the sensor. Using the absorption line of ammonia at 6528.76 cm^{-1}, a minimum detectable absorption coefficient of approximately 1×10^{-8} cm^{-1} is demonstrated for 256 averages. This is achieved for a 1.4-km absorption path length and a 2-s data-acquisition time. These results yield a detection sensitivity of approximately 8.6×10^{-10} cm^{-1} $Hz^{-1/2}$. Ammonia in exhaled breath is analyzed and found in a concentration of 870 ppb for our example. [DOI: 10.1117/1.JBO.20.3.037001]

Keywords: breath analysis; cavity-enhanced absorption spectroscopy.

Paper 150003R received Jan. 2, 2015; accepted for publication Feb. 18, 2015; published online Mar. 5, 2015.

1 Introduction

Analysis of the concentrations of volatile organic compounds (VOCs) in breath offers many advantages over the existing serum or urine analysis, such as being noninvasive, easily repeated, and a painlessness procedure. Because the production of VOCs in breath can be affected by metabolic disorders or diseases, the breath analysis can provide an intrinsically safe method with great potential for disease diagnostics and metabolic status monitoring. Therefore, breath analysis has attracted a considerable attention in scientific and clinical studies. To date, more than 1000 trace VOCs have been found to be present in exhaled breath at concentrations from the ppmv to pptv range. The VOCs in the exhaled breath can be established as biomarkers for particular diseases and metabolic disorders.[1] Breath analysis has a long history. Despite the long investigation time, breath analysis has not yet been introduced as a standard tool in clinical diagnosis. Some problems should be addressed before using breath analysis as a routine tool in the hospitals. Further information on the current status of clinical breath analysis can be found in review articles.[2,3]

Breath analysis can be implemented by different techniques, such as gas chromatography mass spectrometry (GC-MS), selected ion flow tube mass spectrometry (SIFT-MS), proton transfer reaction mass spectrometry, and laser-based sensor. So far, one of the most used techniques for breath gas analysis is the GC-MS. But this method has several disadvantages: expensive, bulky, needs complicated procedures for sample collection, and preconcentration. For breath analysis and its practical applications in hospitals, the parameters such as high sensitivity, selectivity, low-response time, low-detection limit, robustness, cost, size, real-time, and point-of-care detection are important. Because the laser-based techniques such as tunable diode laser absorption spectroscopy,[4] cavity ringdown spectroscopy (CRDS),[5] integrated cavity output spectroscopy (ICOS),[6] cavity-enhanced absorption spectroscopy (CEAS),[7] photoacoustic spectroscopy (PAS),[8] quartz-enhanced photoacoustic spectroscopy,[9] can provide these features, it is an excellent method for analyzing the VOCs in exhaled breath. One of the most popular is OA CEAS. The ICOS and CEAS are the same method. ICOS is used in the context of pulsed excitation and CEAS is used in the context of CW cavity excitation. CEAS was first demonstrated by Engeln et al. in 1998,[10] and ICOS by O'Keefe et al. in the same year.[11,12] These methods are based on the analysis the intensity of light transmitted through a high finesse optical cavity as a function of wavelength. In the off-axis alignment, the laser beam is coupled into the optical cavity at a small angle with respect to the cavity axis or away from the central axis of the optical cavity. In this way, the beam has a longer path length before it reaches its reentrant condition and begins to overlap with itself, resulting in the excitation of an extremely dense mode spectrum.[13] The reentrant condition requires the satisfying of the equation $2m\beta = 2n\pi$, where m is the number of optical round-trip passes, $\cos \beta = 1 - L/r$, L is

*Address all correspondence to: Ismail Bayrakli, E-mail: ismailbayrakli@sdu.edu.tr

1083-3668/2015/$25.00

the cavity length, r is the radius of the mirror curvature, and n is an integer. The effective free spectral range (FSR) of the optical cavity is $c/2mL$, and this decreases with the number of beam round trips. For OA-CEAS, the highest possible value of m is desired without having beam overlaps on the mirror surfaces. A more effective average of the cavity modes can be achieved, leading to the reduction, the etaloning effect, and the saw tooth modulation, thereby to a better signal-to-noise ratio (SNR) compared to the on-axis alignment CEAS.[14] The OA-CEAS has several advantages over CRDS or the multipass cell absorption method: it is almost insensitive to vibrations and to fluctuations in pressure and temperature; there no need for active locking and high-speed electronics. These advantages make the OA-CEAS instrument suitable for measurements outside the laboratory environment.

The detection of biomarkers present in breath requires narrow linewidth (<1 MHz), mode-hop-free (1 to 2 cm^{-1}), wavelength-tunable, single-mode light sources. The external cavity lasers (ECLs) can provide these features. Therefore, these laser types are excellent sources for combination with CEAS methods and for breath analysis. The other sources, such as optical parametric oscillator, difference frequency generator, and CO_2 laser, are bulky, complex, and expensive. In many studies on the ECLs in Littrow, Littman-Metcalf, or other extended configurations, the laser diodes that also operate without any EC configuration are usually used as the gain medium. In such setups, lasing persists simultaneously on both the internal and EC modes for the whole duration of the current pulse toward the low frequency boundary of the gain spectrum.[15] To our knowledge, the tuning range of most ECLs is not very broad due to the gain curve of the used laser diodes (80 to 100 nm).[16,17] Only a few papers have been published on ECLs with a wide tuning range (150 to 200 nm). In most papers, the commercially distributed feedback diode lasers or ECLs are used to analyze VOCs. To our knowledge, only a few studies so far have dealt with developing ECL and CEAS systems together to analyze the VOCs in breath.

One of the VOCs in breath is ammonia, which is established as a biomarker for clinical diagnostics, such as hemodialysis monitoring,[18] diagnosis of hepatic encephalopathy,[19] and detection of Helicobacter pylori.[20] Aguilar et al observed the normal physiological range for human breath ammonia in the region of 50 to 2000 ppb using electrically conducting polymer nanojunctions.[21] Diskin et al demonstrated the mean concentrations of ammonia between 422 and 2389 ppb using SIFT-MS.[22] In Table 1, some parameters for a variety of published laser-based ammonia detection experiments are listed to compare to this and other related work. Our results are better than the results of many other reported studies. Some publications demonstrate better results than our results. But these methods are expensive, complex, and use bulky lasers and/or are combined with other methods, such as wavelength modulation spectroscopy. It should be, however, noted that the use of different expressions of sensitivities for evaluating performance, such as noise equivalent absorption sensitivity, minimum detectable absorption coefficient, and work by different authors makes it difficult to compare the spectroscopic instruments and experiments.[23]

In this work, we demonstrate a breath sensor based on an OA-CEAS and an ECL using an amplitude stabilizer. First, a narrow-linewidth, ultrabroadly coarse (170 nm, 720 cm^{-1}), and fine (1.85 cm^{-1}) wavelength-tunable, single-mode, high output power (100 mW) ECL using a gain chip on a thermoelectric cooler (TEC) for the spectral range between 6890 cm^{-1} (1451 nm) and 6170 cm^{-1} (1621 nm) is demonstrated. The used gain chip has an angled waveguide, AR coating, a broader gain bandwidth, and does not lase without any external cavity setup. In our ECL setup, there is only one EC mode (single-mode operation) over the whole gain spectrum. Therefore, our ECL is well suited for broadband high-resolution spectroscopy. The light emitted from this laser is coupled into the optical cavity formed by two 25.4 mm high-reflective (>99.96% over the spectral range between 700 and 1650 nm) mirrors, in order to analyze the biomarkers in breath. The upper limit of the linewidth of our ECL is measured by using the optical cavity, and is found to be ~140 kHz. Our system is able to detect any molecules in breath at concentrations to the ppbv range that have absorption lines in the spectral range between 1450 and 1620 nm. The performance of the sensor is evaluated with ammonia selected as the target molecule. Using the absorption line of ammonia at 6528.76 cm^{-1}, a minimum detectable absorption coefficient (α_{min}) of approximately 1×10^{-8} cm^{-1} is obtained for 256 averages. This is achieved for a 1.4-km

Table 1 Some parameters for a variety of published laser-based ammonia detection experiments. (N)NEAS: (normalized) noise equivalent absorption sensitivity, MDAC: minimum detectable absorption coefficient, CEDCS: cavity-enhanced dual-comb spectroscopy, QCL: quantum casade laser, DFB DL: distributed feedback diode laser, MLFL: mode-locked fiber laser, OFCS: optical frequency comb spectroscopy.

Methods	(N)NEAS, MDAC	Wavelength (μm)	References
CEDCS	1.0×10^{-10} cm^{-1} $Hz^{-1/2}$	1	24
ECL + OA CEAS	8.6×10^{-10} cm^{-1} $Hz^{-1/2}$	1.53	This work
DFB QCL + CRDS	3.4×10^{-9} cm^{-1} $Hz^{-1/2}$	8.5	25
DFB QCL + WMS	2.0×10^{-7} cm^{-1} $Hz^{-1/2}$	9	26
DFB DL + QEPAS	7.2×10^{-9} cm^{-1} $WHz^{-1/2}$	1.53	27
DFB DL + QEPAS	8.9×10^{-9} cm^{-1} $WHz^{-1/2}$	2	28
MLFL + OFCS	8.0×10^{-10} cm^{-1}	1.5	29
CO_2 Laser + PAS	9.6×10^{-10} cm^{-1}	10	30

absorption path length and a 2-s data-acquisition time. These results yield a detection sensitivity of approximately 8.6×10^{-10} cm^{-1} Hz$^{-1/2}$. To show the suitability of our developed setup for real-time human exhaled breath measurements, ammonia in exhaled breath is analyzed and found in a concentration of 870 ppb for our example.

2 Experimental Setup

Our experimental setup is shown in Fig. 1. We first established and characterized the ECL system. Then the laser is combined with an OA-CEAS technique to analyze the biomarkers in breath. In the following, our ECL, OA-CEAS, and NH_3 breath analyses are described.

2.1 *External Cavity Laser*

The experimental setup of our ECL is arranged in a Littrow configuration (Fig. 1). A gain chip on a TEC cooler (Thorlabs, SAF1550S2) is used as the gain medium. The gain chip does not lase without any external cavity setup. The coupling facet of the gain chip has a reflection coefficient of 0.005% due to the angled waveguide (26.5 deg) and AR coating. This feature suppresses the Fabry-Perot (FP) chip modes, and minimizes the interference between cavities which can prevent fine tuning. The optical isolator on the fiber output protects the chip against back reflections and improves the stability of the laser. The gain chip is installed on a manual precision rotation stage (Thorlabs, PR01/M) and is driven by a laser driver/TEC controller (Thorlabs, ITC4005) in CW mode. To collimate the beam from the gain chip, an AR coated aspheric lens with an 8-mm focal length and NA = 0.5 (Thorlabs, A240TM-C) is used. The lens is mounted on a motorized XYZ stage with picomotor actuators (Newport, 9062-XYZ-PPP-M, 8763-KIT). Then, the collimated beam is oriented TM-polarized to a diffraction grating (Thorlabs, 1050 grooves/mm, 1550 nm) having high diffraction efficiency. The grating is used as a band-pass filter and is installed on a piezo driven rotation stage (Newport, AG-PR100V6, AG-UC8). The rotation stage features a 360 deg continuous rotation and has a minimum incremental motion of 5 μrad (1 arcsec). The distance between the outcoupling facet and grating is approximately 7 cm. The first order of the diffracted beam provided the optical feedback. The selected mode is coupled back into the gain chip and is amplified. The operation from one mode to another mode is achieved by altering the grating angle with respect to the incident beam. Output power is amplified to 100 mW using an optical amplifier (Thorlabs, S9FC1004P). All components are mounted on a stainless steel heavy base plate.

The output is taken from the fiber output and directed to a monochromator system (Newport Cornerstone 130 1/8 m, 200-5000 nm) for taking the spectra. In Fig. 2, the measured spectra of the ECL at different grating angles are shown. An ultra-broadly coarse wavelength tuning range of 720 cm^{-1} (170 nm) for the spectral range between 6890 cm^{-1} (1451 nm) and 6170 cm^{-1} (1621 nm) is achieved by rotating the diffraction grating forming an ECL configuration in single-mode operation. The tuning range is limited by the gain bandwidth of the gain medium.[31] The spectra are taken at the injection current of 300 mA at $T = 23$°C. The maximum side mode suppression ratio is greater than 20 dB.

The mode-hop tuning becomes possible by rotating the grating. When the laser is tuned, the distance l between the gain chip and the grating is not varied. Therefore, mode hopping is obtained on the FP modes of the extended cavity separated by $1/2(n_g L + l)$ ~0.068 cm^{-1} (The FP modes of the gain chip are separated by $1/2n_g L$ ~1.56 cm^{-1}, L: chip length = 1 mm).

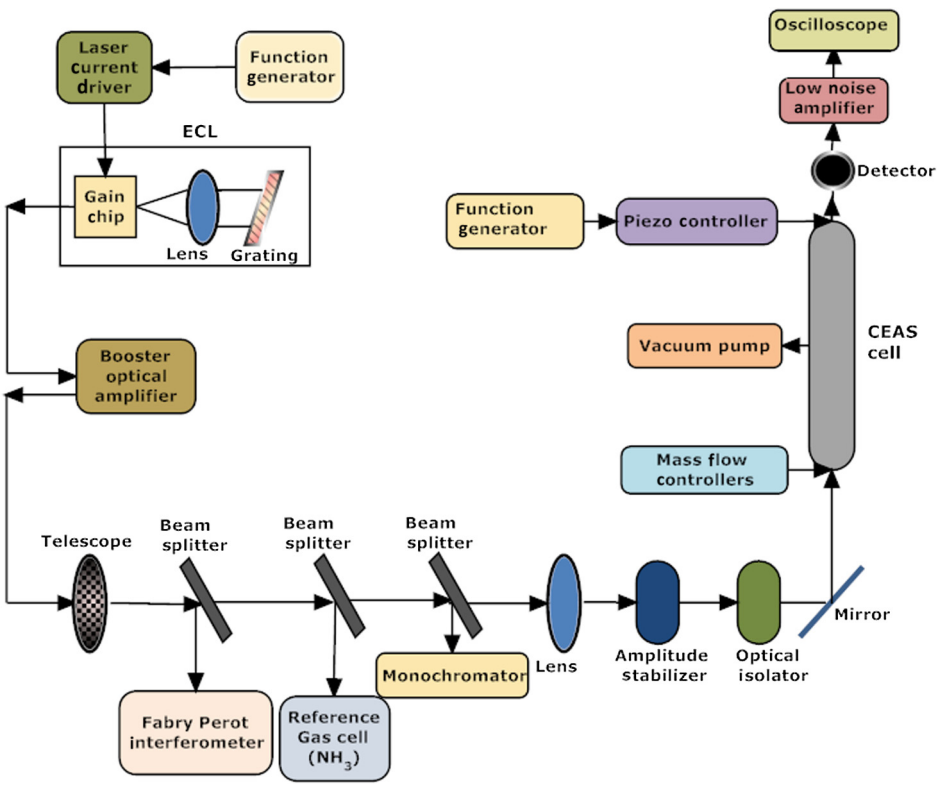

Fig. 1 Experimental setup.

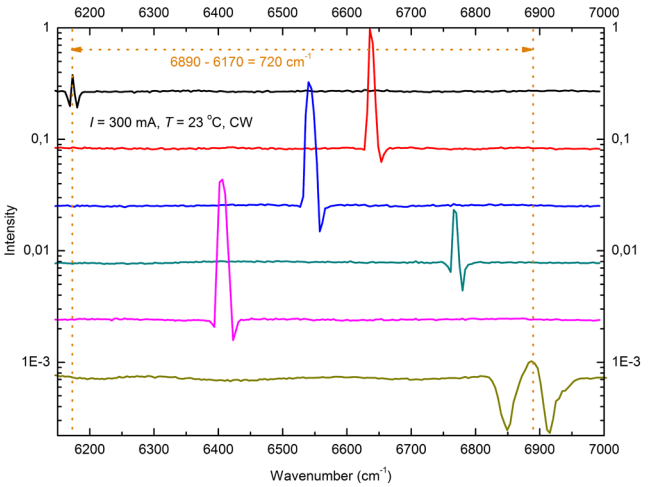

Fig. 2 Measured spectra from coarse grating tuning between 1451 and 1621 nm in single-mode operation.

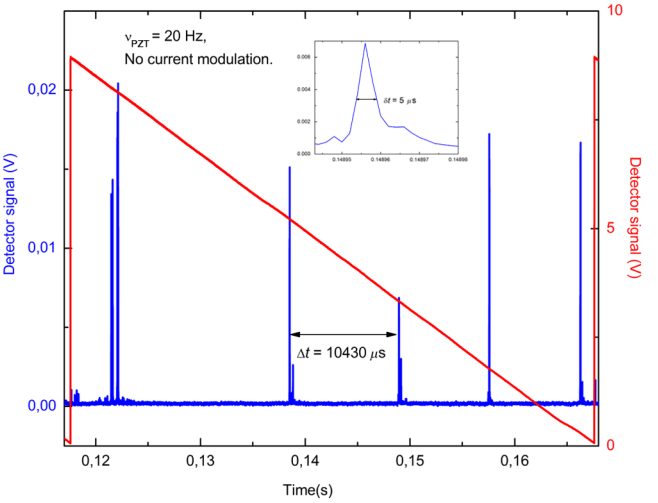

Fig. 4 The linewidth measurement by an optical cavity. Spikes observed during one period of the cavity length modulation with a frequency of 20 Hz. The laser frequency is fixed. The bigger spikes correspond to the TEM_{00} cavity mode, the smaller peaks are due to higher order transverse modes. Uneven spacing of TEM_{00} modes is attributed to the piezoelectric transducer (PZT) nonlinearity.

Simultaneously varying the external cavity length and the injected current makes fine tuning possible. To observe the fine tuning behavior, the resolution of our monochromator is not sufficient. For this purpose, an unbiased (no scanning) FPinterferometer (FPI) (Thorlabs, SA201-EC, SA200-12B, 0.05 cm^{-1} FSR), a cell filled with NH_3, an InGaAs fixed gain detector (Thorlabs, PDA10CF-EC), and an oscilloscope (Tektronix, DPO3034) are used. In Fig. 3(a), the laser power transmitted through the NH_3 cell and the peaks from FPI are shown. The power without the cell is also depicted in this figure. Because the absorption lines of NH_3 are clearly visible, we can deduce that fine tuning is possible. The single-mode operation is shown by using a biased (scanning) FPI (Thorlabs, SA201-EC, SA200-12B, 0.05 cm^{-1} FSR). In Fig. 3(b), the results taken at the different injection current values are shown. No extra peak within the FSR is observed, showing the single-mode operation.

An optical cavity formed by two highly reflective mirrors (described below) can provide a greater resolution for the linewidth measurement as compared to the monochromator. The width of an individual spike in Fig. 4 enables us to evaluate the laser linewidth, because it represents the time required for a moving cavity mode to cross the laser line.[32] From the equation $\Delta\nu_{\text{line}}/\text{FSR} = \Delta t(\text{Spike})/\Delta t(\text{FSR})$, the upper limit for the linewidth of our ECL is found to be approximately 140 kHz (4.7×10^{-6} cm^{-1}), where the FSR of the cavity in on-axis alignment = 300 MHz (0,01 cm^{-1}), $\Delta t(\text{Spike})$ ~5 μs and $\Delta t(\text{FSR})$ ~10430 μs. The spikes in Fig. 4 are observed during one period of the cavity length modulation. The bigger spikes correspond to the TEM_{00} cavity mode, while the smaller peaks are due to higher order transverse modes. The uneven spacing of TEM_{00} modes is attributed to the piezoelectric transducer (PZT) nonlinearity. It should be noted that no amplifier is used for this measurement.

2.2 *Off-Axis Cavity-Enhanced Absorption Spectroscopy*

The laser beam is coupled into the CEAS cavity in the OA alignment via a 50 cm lens and a mirror. The cavity consists of two highly reflective mirrors positioned 50 cm apart with a

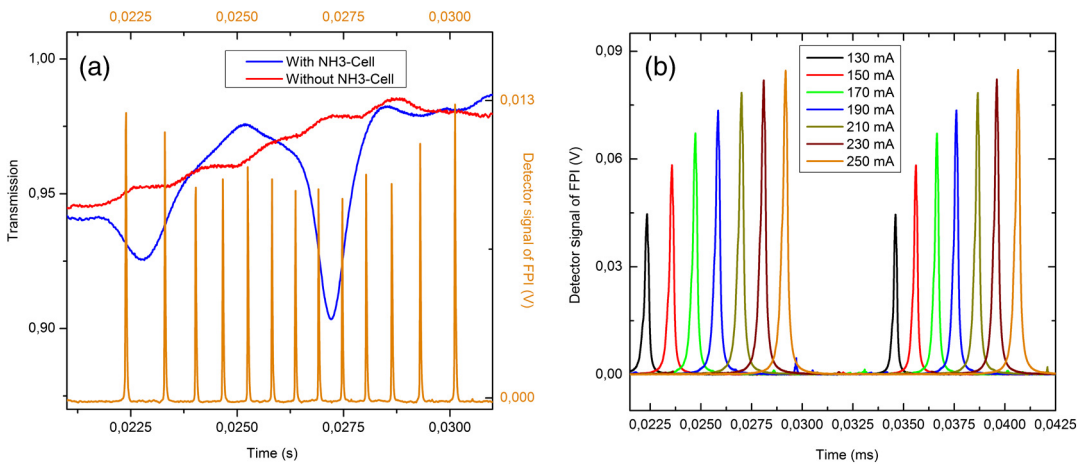

Fig. 3 (a) Laser power with and without an NH_3 cell. The absorption lines of NH_3 are clearly seen. The Fabry-Perot interferometer (FPI) peaks are also shown. (b) Single-mode operation at different injection current values.

reflectivity of >99.96% over the spectral range between 700 and 1650 nm with a 2.54 cm diameter and a radius of curvature of 1 m (LayerTec GmbH). The cavity modes are obtained by scanning the cavity length by generating a sawtooth wave at 10 Hz using a function generator (Tektronix, AFG3021B) and a three-channel piezo controller (Thorlabs, MDT693B) modulating the three piezoelectric transducers (Thorlabs, PE4), while keeping the laser frequency fixed. The radiation exiting the cavity is focused on an InGaAs fixed gain detector (Thorlabs, PDA10CF-EC) with DC from a 150-MHz bandwidth. After amplification (gain factor: 10^3) and filtering (30 kHz low filter) by a low-noise amplifier (SRS, SR560), the signal is fed to a digitizing oscilloscope (Tektronix, DPO3034). The oscilloscope output is connected to a computer via USB connection and recorded using Tektronix analysis software. The transmitted intensity through the cavity for OA alignment is depicted in Fig. 5 while keeping the laser frequency fixed.

Relative frequency calibration is achieved by passing the laser light through an FPI with a free spectral range (FSR) of 1.5 GHz (0.05 cm^{-1}). The transmitted light is focused by a lens onto an InGaAs fixed gain detector. Absolute frequency calibration is performed with a reference gas cell containing NH_3. To insert the gas into the CEAS cavity and to evacuate from the cavity, a mass flow controller (Alicat, MCV-2SLPM-D/5M) and a vacuum pump (Agilent, IDP3) are used. The pressure inside the cavity is measured with a vacuum gage (Agillent, PCG-750).

The cavity provides a linear absorption signal gain if the condition $G\alpha \ll 1$ is satisfied, where $G = R/(1-R)$ is the cavity gain factor.[33] In order to experimentally determine the value of the line strength, the integrated CEAS signal $[(I_0/I)-1]/d$ is plotted as a function of the pressure [Fig. 6(a)]. The slope of the linear fit through the data points gives a value for the line strength of approximately 2.5×10^{-21} cm^{-1}/molecule cm^{-2} for the absorption line at 6528.76 cm^{-1}, which is in agreement with the result reported by Webber et al.[34]

To calibrate the mirror reflectivity for quantitative analysis, the integrated absorption $[(I_0/I)-1]/d$ is plotted as a function of the NH_3 concentration [Fig. 6(b)] on the basis of Eq. (1). A mirror reflectivity can be determined from the slope of the resulting liner fit using Eq. (1). From these measurements, the mirror reflectivity R of 0.99964 ± 0.00001 is determined, which corresponds to an effective path length (L_{eff}) of 1.4 ± 0.001 km.

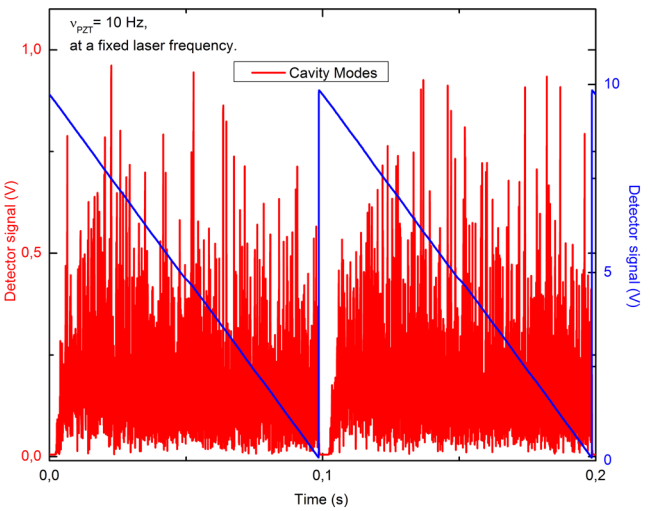

Fig. 5 Transmitted intensity through the off-axis cavity-enhanced absorption spectroscopy (OA-CEAS) cell (cavity modes) at a fixed laser frequency.

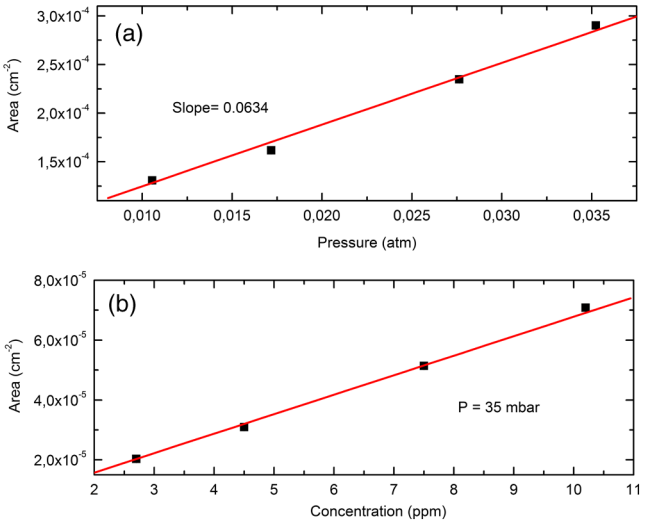

Fig. 6 (a) The integrated cavity-enhanced absorption spectroscopy (CEAS) signal as a function of the pressure. The slope of the linear fit through the data points gives a value for S of 2.5×10^{-21} cm^{-1}/molecule cm^{-2}. (b) The integrated CEAS signal as a function of the NH_3 concentration is shown. The slope of the linear fit through the data points gives a value for R of 0.99964 ± 0.00001.

In Fig. 7(a), the transmission signal through the CEAS cell filled with 2.7 ppm NH_3 in N_2 is shown. A 2.7-ppm concentration is generated by inserting a certified mixture containing 96 ppm of NH_3 buffered in N_2 (Linde) in the cell to a pressure of 2.86 mbar and then pure N_2 gas is added to reach a total pressure of 1000 mbar. After reducing the pressure of the cell to 35 mbar, spectra are obtained by scanning the laser frequency by generating a sine wave at 120 Hz using a piezo controller (Thorlabs, MDT693B) modulating the PZT controlling the external cavity grating and typically averaging 256 scans with an oscilloscope (Tektronix, DPO3034). To smooth the cavity resonance spikes, many laser frequency scans are averaged. The absorption coefficient, which is calculated according to Eq. (1), and Voigt fits through the experimental data points are depicted in Fig. 7(b).

$$\alpha = \left(\frac{I_0}{I} - 1\right)\left(\frac{1-R}{d}\right), \tag{1}$$

where I_0 is the baseline signal, I is the recorded CEAS signal, R is the reflectivity of the cavity mirrors, and d is the distance between the cavity mirrors.

For ammonia detection, a minimum detectable absorption coefficient (α_{min}) of approximately 1×10^{-8} cm^{-1} is obtained for 256 averages using the absorption line at 6528.76 cm^{-1}. This is achieved for a 1.4-km absorption path length and a 2-s data acquisition time. The noise equivalent absorption sensitivity (NEAS) is calculated from the minimum detectable absorption coefficient and detection bandwidth. The detection bandwidth is defined as the cavity bandwidth [$f_{cavity} = 1/(2\pi\tau)$] divided by the number of sweeps averaged. A detection bandwidth of approximately 135.2 Hz is estimated

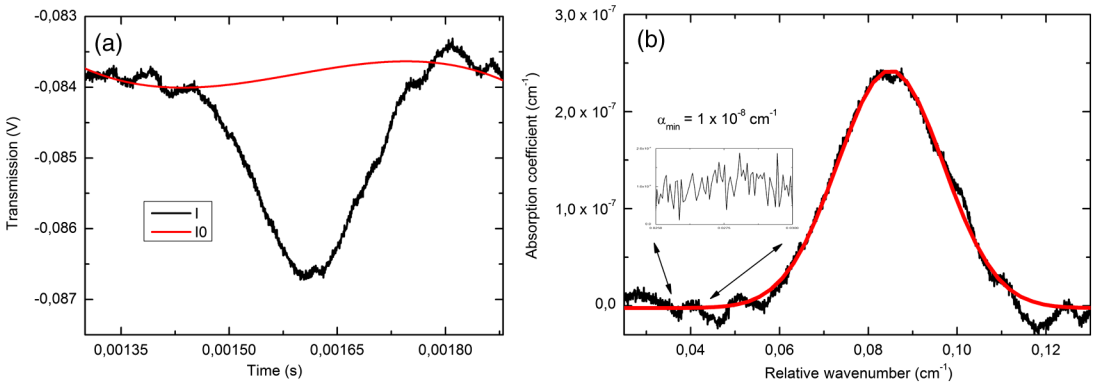

Fig. 7 (a) Transmission signal through the CEAS cell filled with 2.7-ppm NH_3 in N_2. (b) Absorption coefficient.

(τ ~4.6 μs, f_{cavity} ~34.6 kHz, 256-sweep average). From these results, a noise equivalent absorption sensitivity of approximately 8.6×10^{-1} cm^{-1} Hz$^{-1/2}$ is obtained. This result is better than the results of many other publications, but is worse than the results of some studies. For example, in Ref. 24, NEAS is found to be 1.0×10^{-10} cm^{-1} Hz$^{-1/2}$ using cavity-enhanced dual-comb spectroscopy at 1 μm. This is an eight times factor better than our work. But the setup is more complex and expensive than our setup. It should be, however, noted that the comparisons of spectroscopic instruments and experiments are difficult due to the use of different metrics for evaluating performances by different authors.[23]

The cavity mode-noise resulting from the relative intensity fluctuations can be reduced by using OA alignment. For OA-ICOS, it is desired to achieve a significantly smaller effective FSR than the laser linewidth. In such a case, the resonant cavity properties can be eliminated and the cavity output does not depend on laser frequency, reducing the noise caused by the transmission variations as the laser scans from mode to mode. However, a narrow laser bandwidth makes it difficult to narrow the FSR small enough. Instead, one of the cavity mirrors can be dithered and/or the laser frequency can be scanned through the cavity mode. Therefore, one mirror of the optical cavity is dithered with three piezo actuators (Thorlabs, PE4), resulting in a better mode average and thereby in a better SNR. An amplitude stabilizer (Thorlabs, LCC3113H/M) positioned in front of the optical cavity is used to further improve the SNR, and thus, the detection limit. A 43-dB optical isolator (Thorlabs, IOT-4-1550-VLP) is used to prevent back reflection from the optical cavity.

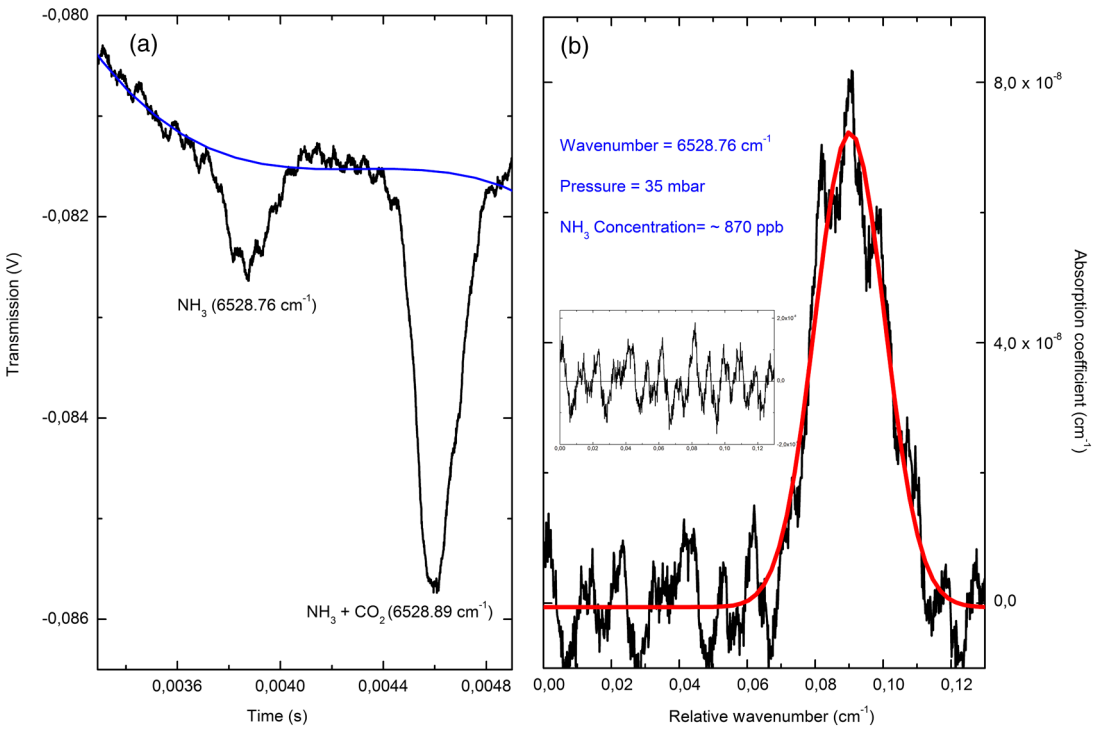

Fig. 8 (a) Transmission signal through the CEAS cell filled with breath. The isolated absorption line of NH_3 at 6528.76 cm^{-1} and the absorption line of NH_3 and CO_2 at 6528.89 cm^{-1} are shown. (b) The absorption coefficient of NH_3 at 6528.76 cm^{-1}.

2.3 *Breath Analysis*

To show the suitability of our developed setup for ultrasensitive real-time human exhaled breath measurements, ammonia in exhaled breath is analyzed. The NH_3 absorption line at 6528.76 cm^{-1} is an isolated line and is suitable for breath analysis. The following procedures for breath analysis are done to remove the residual ammonia in the cell and to prepare the system for the next sample: before taking measurements, the cell is evacuated by a vacuum pump (Agilent, IDP3) to an achievable minimum value (approximately 7×10^{-2} mbar). After filling the cell with pure N_2 to a total pressure of 1000 mbar, it is again evacuated. This procedure is repeated, until no significant signal is observed (typically 3 to 4 times). The cell is heated to 35 to 40°C for desorption of ammonia adhered on the mirror surfaces and walls of the cell. The measurement is carried out at a reduced pressure of 35 mbar.

The alveolar air sample is collected by using a mouthpiece, flutter valve, tee connector, collection bag, and discard bag (Quintron). The separation of the dead-space air from alveolar air is performed by using the disposable polyethylene discard bag. The expired breath air, containing "dead-space" air, is first directed into the discard bag, and then the alveolar air is diverted into the collection bag. To deliver the alveolar air sample collected in the collection bag into the cell, a two-way non-rebreathing valve (Hans Rudolph Inc.) and a mass flow controller calibrated for exhaled breath (Alicat, MCV-2SLPM-D/5M) are used. The transmission signal through the CEAS cell filled with alveolar air is depicted in Fig. 8(a). From this figure, the isolated absorption line of NH_3 at 6528.76 cm^{-1} and the absorption line of NH_3 and CO_2 at 6528.89 cm^{-1} can be seen. In Fig 8(b), the absorption coefficient of NH_3 at 6528.76 cm^{-1} is shown. Ammonia in breath is found in a concentration of 870 ppb for our example.

3 Conclusion and Outlook

In conclusion, a biomedical sensor based on an OA-CEAS using a room temperature ECL and an amplitude stabilizer is reported and the ability to measure the VOCs in breath is demonstrated. A high-power, single-mode, narrow linewidth, and widely wavelength-tunable continuous wave ECL using a gain chip on a TEC is demonstrated. A broadly coarse wavelength tuning range of 720 cm^{-1} (170 nm) for the spectral range between 6890 cm^{-1} (1451 nm) and 6170 cm^{-1} (1621 nm) is achieved by rotating the diffraction grating. A mode-hop-free tuning range of 1.85 cm^{-1} is obtained by simultaneously varying the external cavity length and the injection current. A PZT with a higher displacement and/or a larger injection current ramp can increase the fine tuning range. The upper limit of the linewidth of our ECL is determined to be approximately 140 kHz. Any biomarker in breath at concentrations to the ppbv range which has a suitable absorption line in the spectral range between 1450 and 1620 nm can be analyzed with our developed sensor. Ammonia is selected as the target molecule to evaluate the performance of the sensor. Using the absorption line of ammonia at 6528.76 cm^{-1}, a minimum detectable absorption coefficient (α_{min}) of approximately 1×10^{-8} cm^{-1} over an effective optical length of 1.4 km is obtained for 256 averages. This is achieved for a 2-s data acquisition time. These results yield a noise equivalent absorption sensitivity of approximately 8.6×10^{-10} cm^{-1} $Hz^{-1/2}$. Ammonia in exhaled breath is analyzed and found in a concentration of 870 ppb for our example.

Acknowledgments

This work was supported by the Scientific and Technological Research Council of Turkey (TUBITAK, 112E559).

References

1. C. Wang and P. Sahay, "Breath analysis using laser spectroscopic techniques: breath biomarkers, spectral fingerprints, and detection limits," *Sensors* **9**, 8230–8262 (2009).
2. T. H. Risby and F. K. Tittel, "Current status of midinfrared quantum and interband cascade lasers for clinical breath analysis," *Opt. Eng.* **49**(11), 111123 (2010).
3. T. H. Risby and S. F. Solga, "Current status of clinical breath analysis," *Appl. Phys. B* **85**, 421–426 (2006).
4. D. S. Baer et al., "Multiplexed diode-laser sensor system for simultaneous H2O, O2, and temperature measurements," *Opt. Lett.* **19**, 1900–1902 (1994).
5. M. Mazurenka et al., "Cavity ring-down and cavity enhanced spectroscopy using diode lasers," *Annu. Rep. Prog. Chem. Sect. C: Phys. Chem.* **101**, 100–142 (2005).
6. D. S. Baer et al., "Sensitive absorption measurements in the near-infrared region using off-axis integrated-cavity-output spectroscopy," *Appl. Phys. B: Lasers Opt.* **75**, 261–265 (2002).
7. R. Peeters et al., "Open-path trace gas detection of ammonia based on cavity-enhanced absorption spectroscopy," *Appl. Phys. B: Lasers Opt.* **71**, 231–236 (2000).
8. D. Hofstetter et al., "Photoacoustic spectroscopy with quantum cascade distributed-feedback lasers," *Opt. Lett.* **26**, 887–889 (2001).
9. A. A. Kosterev et al., "Quartz-enhanced photoacoustic spectroscopy," *Opt. Lett.* **27**, 1902–1904 (2002).
10. R. Engeln et al., "Cavity enhanced absorption and cavity enhanced magnetic rotation spectroscopy," *Rev. Sci. Instrum.* **69**, 3763 (1998).
11. A. O'Keefe, J. J. Scherer, and J. B. Paul, "CW integrated cavity output spectroscopy," *Chem. Phys. Lett.* **307**, 343–349 (1999).
12. A. O'Keefe, "Integrated cavity output analysis of ultra-weak absorption," *Chem. Phys. Lett.* **293**, 331 (1998).
13. G. S. Engel et al., "Ultrasensitive near-infrared integrated cavity output spectroscopy technique for detection of CO at 1.57 μm: new sensitivity limits for absorption measurements in passive optical cavities," *Appl. Opt.* **45**(36), 9221–9229 (2006).
14. W. Zhao et al., "Wavelength modulated off-axis integrated cavity output spectroscopy in the near infrared," *Appl. Phys. B* **86**, 353–359 (2007).
15. B. Hinkov et al., "Time-resolved characterization of external-cavity quantum-cascade lasers," *Appl. Phys. Lett.* **94**, 221105, (2009).
16. L. Hildebrandt et al., "Antireflection-coated blue GaN laser diodes in an external cavity and Doppler-free indium absorption spectroscopy," *Appl. Opt.* **42**, 2110–2118 (2003).
17. E. Geerlings et al., "Widely tunable GaSb-based external cavity diode laser emitting around 2.3 μm," *IEEE Photon. Technol. Lett.* **18**, 1913–1915 (2006).
18. L. R. Narasimhan, W. Goodman, and C. K. Patel, "Correlation of breath ammonia with blood urea nitrogen and creatinine during hemodialysis," *Proc. Natl. Acad. Sci. U. S. Am.* **98**(8), 4617–4621 (2001).
19. S. DuBois et al., "Breath ammonia testing for diagnosis of hepatic encephalopathy," *Dig. Dis. Sci.* **50**(10), 1780–1784 (2005).
20. D. J. Kearney, T. Hubbard, and D. Putnam, "Breath ammonia measurement in helicobacter pylori infection," *Dig. Dis. Sci.* **47**(11), 2523–2530 (2002).
21. A. D. Aguilar et al., "A breath ammonia sensor based on conducting polymer nanojunctions," *IEEE Sens. J.* **8**(3), 269–273 (2008).
22. A. M. Diskin, P. Spanel, and D. Smith, "Time variation of ammonia, acetone, isoprene and ethanol in breath: a quantitative SIFT-MS study over 30 days," *Physiol. Meas.* **24**(1), 107–19 (2003).
23. E. J. Moyer et al., "Design considerations in high-sensitivity off-axis integrated cavity output spectroscopy," *Appl. Phys. B* **92**, 3, 467–474 (2008).
24. B. Bernhardt et al., "Cavity-enhanced dual-comb spectroscopy," *Nat. Photonics* **4**, 1, 55–57 (2009).
25. B. A. Paldus et al., "Cavity ringdown spectroscopy using mid-infrared quantum-cascade lasers," *Opt. Lett.* **25**(9), 666–668 (2000).

26. D. Weidmann et al., "Mid-infrared trace-gas sensing with a quasi-continuous-wave Peltier-cooled distributed feedback quantum cascade laser," *Appl. Phys. B: Lasers Opt.* **79**(7), 907–913 (2004).
27. A. A. Kosterev and F. K. Tittel, "Ammonia detection by use of quartz-enhanced photoacoustic spectroscopy with a near-IR telecommunication diode laser," *Appl. Opt.* **43**(33), 6213–6217 (2004).
28. R. Lewicki et al., "Carbon dioxide and ammonia detection using 2 μm diode laser based quartz-enhanced photoacoustic spectroscopy," *Appl. Phys. B: Lasers Opt.* **87**(1), 157–162 (2007).
29. M. J. Thorpe et al., "Cavity-enhanced optical frequency comb spectroscopy: application to human breath analysis," *Opt. Express* **16**(4), 2387–2397 (2008).
30. M. B. Pushkarsky, M. E. Webber, and C. K. N. Patel, "Ultra-sensitive ambient ammonia detection using CO2-laser-based photoacoustic spectroscopy," *Appl. Phys. B: Lasers Opt.* **77**(4), 381–385 (2003).
31. I. Bayrakli et al., "Grating-coupled external-cavity short-wavelength ($\lambda \sim 3.9$ μm) InGaAs/InAlAs/AlAs quantum-cascade lasers," *Opt. Quantum Electron.* **41**, 1019–1025 (2009).
32. A. A. Kosterev et al., "Cavity ringdown spectroscopic detection of nitric oxide with a continuous-wave quantum-cascade laser," *Appl. Opt.* **40**(30) (2001).
33. J. B. Paul, L. Lapson, and J. G. Anderson, "Ultrasensitive absorption spectroscopy with a high-finesse optical cavity and off-axis alignment," *Appl. Opt.* **40**(27), 4904–4910 (2001).
34. M. E. Webber, D. S. Baer, and R. K. Hanson, "Ammonia monitoring near 1.5 μm with diode laser absorption sensors," *Appl. Opt.* **40**, 2031–2042 (2001).

Ismail Bayrakli is an assistant professor at Suleyman Demirel University. He received his MSc and PhD degrees in physics from the Technical University of Berlin and Humboldt University, Berlin, Germany, in 2005 and 2008, respectively. His research interests include tunable single- and double-mode diode lasers, ultrasensitive and ultraresolution laser-based biomedical sensors, and breath analysis.

Hatice Akman is a research assistant at Suleyman Demirel University. She received her MSc degree in electronic and telecommunication engineering from Suleyman Demirel University in 2011. Since 2012, she has been a PhD student at Suleyman Demirel University.